2012 14th International Conference on Ground Penetrating Radar (GPR)
June 4-8, 2012, Shanghai, China @ ISBN 978-1-4673-2663-6

Permafrost Soil Water Content Evaluation Using High-Frequency Ground-penetrating Radar in Amdo Catchment, Central Tibetan Plateau

Yingzhao Ma*, Yinsheng Zhang, S.B. Farhan and Yanhong Guo
Key Lab. Of Tibetan Environment Changes and Land Surface Processes
Institute of Tibetan Plateau Research, Chinese Academy of Sciences
Beijing, China
* yzma@itpcas.ac.cn

Abstract — **High-frequency ground-penetrating radar (GPR) was applied to assess soil water content spatially during the freezing periods at a continuous permafrost site in Amdo catchment, which is centrally located in Tibetan Plateau. The active layer thickness was also roughly presented through the whole survey, which traveled almost 15Km from the top of a hill towards a seasonal stream. The results revealed that average soil moisture increased slightly towards the down-slope direction and kept a higher level near the stream, especially in the deeper layers. Moreover, we found that active layer depth varied with topography, and it ranged from 1.92m to 2.44m along the profile. The topography (i.e. slope and elevation) and stream distribution significantly alter spatial pattern of soil moisture and active layer thickness in the study regions.**

Keywords – soil moisture; ground-penetrating radar; Tibetan Plateau; permafrost; active layer depth

I. INTRODUCTION

Ground-penetrating radar (GPR) technique is a geophysical method for subsurface investigations that utilizes electromagnetic signals transmitted into the ground as pulses from an antenna. Compared to other methods, GPR provides the data with high vertical resolution, a potential high recording speed and real-time visualization of the acquired data. Beside that, GPR having the most extensive set of applications for any sort of geophysical study, which is leading to be a wide range of applications in spatial scales and concomitant diversity of instrument configurations. Consequently, high-frequency GPR is applied in various ranges of scientific surveys as a most appropriate technique for detecting sedimentary structures[1], depths of reflecting surfaces such as ground water tables[2], or permafrost tables[3], as well as for evaluating volumetric soil water content [4][5][6], especially in permafrost studies[7].

Soil water content is an important variable in hydrological processes at various spatial scales, which is altered by combination pattern of soil type, topography, rainfall distribution etc. and affects the partitioning of precipitation into infiltration and runoff. GPR is one of the most promising techniques to detect soil moisture at catchment scales, and supplies high-resolution information about the subsurface moisture distribution. The validations and limitations of each GPR method for water content determination have been discussed extensively (e.g. soil moisture identified from reflected wave velocity, ground wave velocity, transmitted wave velocity between boreholes, or surface reflection coefficient)[4], but two important issues should be brought to the forefront. First is about the petrophysical relationship between permittivity and volumetric water content which further requires accurate evaluation with lower-frequency GPR antennas. The other is the sampling volume and spatial resolution of all of the GPR methods, especially under heterogeneous soil conditions [4].

Permafrost on the Tibetan Plateau shows an extremely sensitive response to climate change [8]. Monitoring from boreholes shows an apparently increase in active layer depth, which is a good case in point [8]. Nevertheless, field observation just at point locations (e.g. boreholes) is not fully comprehensive. To develop the understanding of spatial active layer processes in detail, efficient methods allowing a high-resolution mapping of active layer conditions (e.g. soil moisture) are required. In permafrost regions, GPR signal attenuation is relatively high due to the non-penetrable layer beneath active layer. Consequently, successive variability in signal reflection, dispersion and propagation velocity above 100MHz occurs frequently [9], which results in potential venture on monitoring volumetric soil water content in active layers. Moreover, GPR has already been proved effective in estimating soil moisture in permafrost sites, such as Arctic [10] and Tibetan Plateau [11]. After all, there are just a few studies which have been conducted to evaluate soil moisture both spatially and temporally in Tibetan Plateau yet. Multi-channel GPR was once applied at a permafrost site on the Tibetan Plateau to monitor the influence of surface properties and soil texture on the late-summer thaw depth and average soil moisture of the active layer [11], which demonstrated that GPR is an operational technology to study soil water content at an intermediate scales that vary from a few meters to kilometers. The objective of our study was to apply 250MHz high-frequency GPR to effectively estimate spatial distribution of soil moisture in the active layer at a permafrost site during the early freezing periods in central Tibetan Plateau. Beside that, the approximate depths of active layer are presented

laterally across the survey profile, which travels along the hillslope towards a seasonal stream.

II. MATERIALSAND METHODS

A. Field description

The experiment site is located in the Amdo catchment (Fig.1), near the Tanggula Pass and along the Qinghai-Xizang Railway, located in the central Tibetan Plateau. The basin valley is not too large, but much wider that runs from northeast to southwest. A planetary boundary layer (PBL) observation tower was also set up in the watershed, where a soil moisture measurement system (SMMS) was installed at 10 levels from 4 to 279cm below ground surface near the PBL. A seasonal stream runs in the valley, about 6.5km southwest of the town of Amdo (91°37′ E, 32°14′ N, about 4700m above sea level). The average annual precipitation and temperature from 1966 to 2004 was 440 mm and -2.8℃ respectively. Wind along the valley is generally observed to vary diurnally, except when a strong system prevails. The ground surface is essentially bare soil in the pre-monsoon dry season, but is covered with scattered short grasses during the summer monsoon season. The main vegetation in this region is Stipa glareosa, with 10-50% coverage [12]. At the beginning of the monsoon season (late May), the water table is present on the surface, but gradually disappeared in winter. Furthermore, the soil moisture content here increases with depth in the upper 200cm but decreases in the other layers [13].

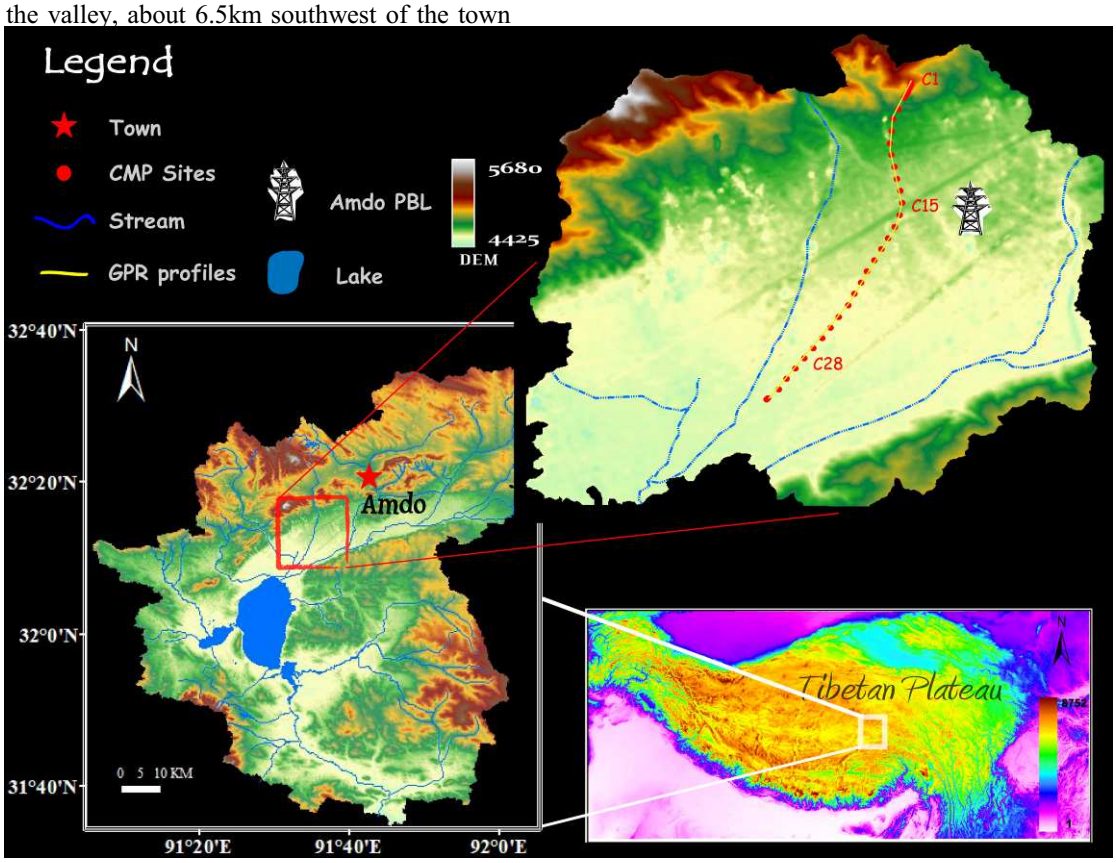

Figure 1. Location of the research site in Amdo, Central Tibetan Plateau

B. Data and analysis

The GPR measurements included a standard reflection profile and thirty-four CMP soundings coincidently collected from the top of a hill to a stream with approximate fifteen kilometers (Fig.1). The reflection line measurement passes through the entire thirty-four CMP soundings rightly. However, only thirty-two CMP soundings were valid for further analysis due to unpredictable noise contamination in the other data. All the GPR data in this study was collected using a Sensors and Software PulseEKKOTM 1000 (Sensors & Software Inc. Mississauga, Ontario, Canada) GPR system equipped with 250MHz shielded antennas. All the readings were measured by a time window of 120 ns, sampling interval of 0.4ns, and 32 stacks per trace. However, the survey was conducted using a step-size of 0.5m for reflection line, but 0.1m increments for CMP data. Data acquisition took place in the early October, 2011, when the surface soil began to freeze in Amdo [13].

We used EKKO View Deluxe software program (Version 1 Release 4, Sensors & Software Inc. Mississauga, Canada) for standard GPR data processing. All data sets were dewowed using the software's default time windows to remove the low-frequency signal saturation arising from the radar equipment. Time-zero drift correction was also incorporated in

each survey. Beside that, band-pass frequency filtering had also been applied with corner frequencies of 50, 100, 500, 750MHz on the raw data. Spreading and exponential compensation (SEC) gains compensated for the spherical spreading losses and the exponential ohmic dissipation of energy in the whole data. Finally, the color density and transparency for each radiogram was adjusted individually for visualization purposes.

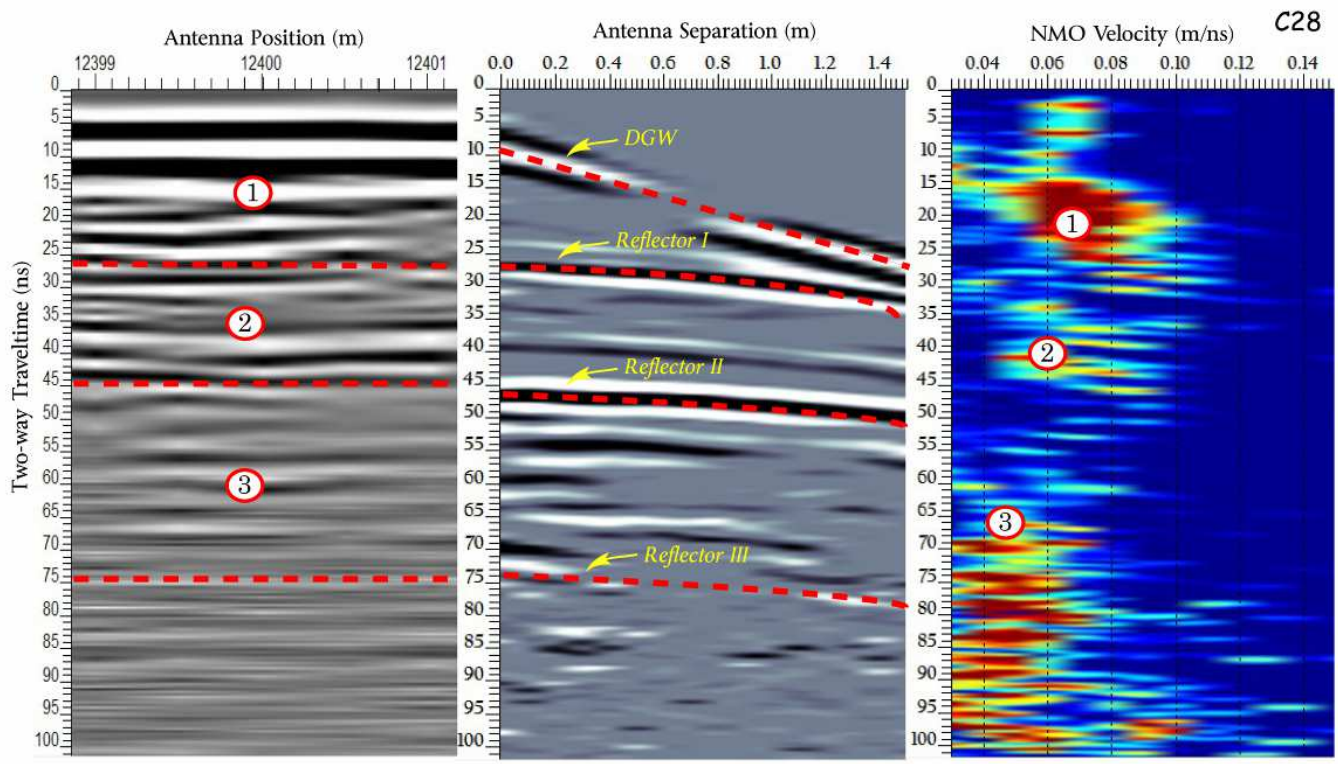

Figure 2. Data processing sequence for a single survey event, where three stratigraphic reflections were identified on 28th CMP site and corresponding reflection profile (in the left) , Direct ground wave (DGW) velocity (in the middle)was determined using least-squares linear analysis while the semblance plot (in the right) was calculated to obtain NMO velocities in each layer.

Interval soil conditions were detected using two-way vertical traveltimes from reflection profiles and NMO velocity analysis of CMP soundings. Compared to reflection method, CMP sounding data is much easier to get reasonable interval wave velocity during variable soil conditions. As a result, strong reflection interfaces and soil dielectric permittivity [1] could be evaluated through velocity analysis of CMP data in each position. Although so many vertical velocity gradients present high levels of uncertainty and may result in bias on the interval layer thickness, we could get relatively precise results of interval depths by averaging the whole CMP data sets. Fig.2 shows three reflection events identified from the survey which was located in the 28th point during CMP observation. Beside that, direct ground wave (DGW) representing shallow surface properties in the upper few decimeters was also labeled, whose velocity was determined by least-squares analysis. Here, we define the upper 0.2m as the thickness of DGW [14]. We also summarized the whole CMP measurements and estimated average interval thickness and corresponding reflection interface depths, which were presented in table I. Considered uncertainties in the measurements on the field and the assumptions in the interpretation and calculations, standard deviation (SD) was also estimated (see table I).

TABLE I. SUMMARY OF AVERAGE TWO-WAY TRAVELTIMES TO REFLECTION EVENTS 1-3 AND INTERVAL THICKNESS AND LOWER INTERFACE DEPTH USING ONE REFLECTION PROFILE AND 32 CMP SOUNDINGS

Depth Interval	Interval Thickness(m)		Lower Interval
	Average	*SD*	*Depth(m)*
DGW	0.20	/	N/A
Interval 1	0.745	0.093	0.75
Interval 2	0.714	0.155	1.46
Interval 3	0.715	0.161	2.18

III. RESULTS AND DISCUSSION

A. Interpretation of common-mid point (CMP) surveys

Fig.3 illustrates the trends of direct ground wave (DGW) and interval 1-3 velocity accompany with corresponding surface topography resulting from 32 CMP soundings. The whole survey can be divided into three parts. The first part is “I”, which ranges from No. 1 to 7 of CMP data and stands for strong hillslope; the second part is “II”, which ranges from No. 8 to 27 of CMP data and delegates slightly weak hillslope; the last one is “III”, which ranges from No.28 to No.32 of CMP data and ends near a seasonal stream (Fig.3). The value of

wave velocity decreases with increasing interval depths in each part. However, the DGW velocity fluctuates more frequently than the interval 1-3 velocities along the whole survey. DGW measurements can be used to monitor and evaluate the formation of a shallow frozen soil layer [1]. Since the observation conducted on early October, while the shallow surface begins to freeze [13], the complicated frozen-unfrozen course caused the heterogeneous in direct ground wave energy. In part I, the velocity in each layer synchronously decrease with lower elevation. While the velocity in each layer keeps relatively stable in part II. Furthermore, the velocity in each layer among part III, locating near a seasonal stream, occurs in a downtrend, especially during the shallow subsurface. Although the water level of the stream is lower in October, the stream may take potential effect on the wave propagation. Beside that, the results demonstrate significant spatial variations of wave velocity in response to changes in soil conditions at different positions and depths.

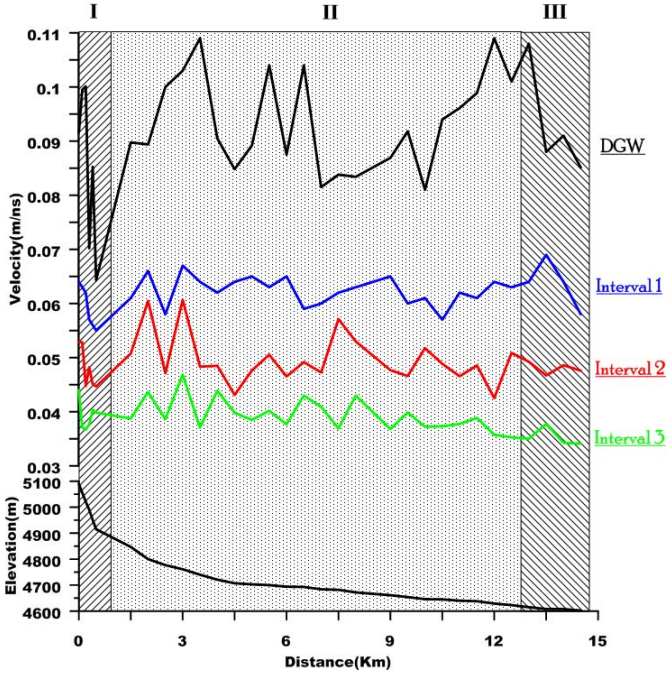

Figure 3. DGW and entire interval velocity accompany with surface topography resulting from 32 CMP sounding data. The entire survey would be devided into three parts. The first part is "I", which ranges from No. 1 to 7 of CMP data and stands for strong hillslope; the second part is "II", which ranges from No. 8 to 27 of CMP data and delegates slightly weak hillslope; the last one is "III", which ranges from No. 28 to 32 of CMP data and relates to a seasonal stream.

B. Evaluation of soil water content

Soil water content estimation from velocity requires a petrophysical relationship to convert the relatively soil permittivity ε into volumetric soil moisture measurement θ. For better illustration soil water content within the defined soil intervals, Topper et al's empirical equation [16] and CRIM (Complex Refractive Index Method) formula [17] were used together in our study, with assuming a porosity of 0.39 and a dielectric permittivity of the solid materials of 5. Fig.4 demonstrates DGW and interval 1-3 moisture variations by the above mentioned two methods, where the dotted line represents CRIM formula, and solid line stands for the other equation. DGW and Interval 1 moisture reflect the shallow soil moisture conditions, while interval 2 and 3 for the deeper levels. Soil moistures in each layer calculated by two different methods, which are almost coincide with each other, especially in the shallow surface (DGW and Interval I). Typically, water is not distributed uniformly in different depths. Soil water content increases with depth in each site. Initially, we expect groundwater to be the principle factor determining the observed higher soil moisture of deeper interval. Whereas the evaportranspiration and root water undertaking in the shallow surface [11] may be the important reasons for lower amount of moisture in the experiment. Furthermore, soil moisture in different interval shows a high spatial variability throughout the whole plots which can be related to the observed differences in soil textural and surface properties. Considering the slope and neighbored stream effect, average soil moisture contents increases slightly towards the downslope (part I) and keep a higher level near the streams (part III), especially in the deeper place. Groundwater would accumulate in the bottom valley gradually, which explains the relatively higher soil moisture contents in the lower elevation to some extent [18].

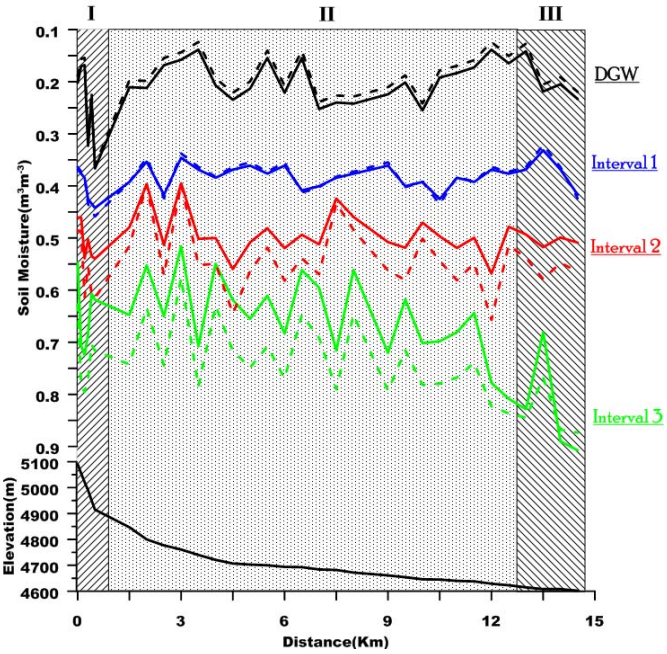

Figure 4. Estimated volumetric water content corresponding to DGW and interval 1-3 velocity measurements. The solid line represents, the Topper et al's empirical equation while the dotted line stands for CRIM method. The entire survey would be devided into three parts. The first part is "I", which ranges from No. 1 to 7 of CMP data and stands for strong hillslope; the second part is "II", which ranges from No. 8 to 27 of CMP data and delegates slightly weak hillslope; the last one is "III", which ranges from No. 28 to 32 of CMP data and relates to a seasonal stream.

C. Predict active layer thickness during the early freezing periods

Permafrost is defined exclusively in physical terms, based on a temperature criterion [19][20], where ground (soil or rock, included ice and organic material) remains at or below 0℃ for at least two consecutive years [21]. Whereas in cold regions, active layer is labeled as "the layer of ground that is subject to

annual thawing and freezing in areas underlain by permafrost" [21]. The thaw depth of the active layer determines the partitioning of surface and ground water runoff and influences the rate of water and gas exchange between the soil and the atmosphere. In Tibetan region, the distribution of active layer depth was deduced from plot scale observations like borehole, as it was concluded to be 2.0-3.0m in the Tanggula mountainous [22]. In order to obtain a better elucidation of active layer processes in spatial, efficient methods (i.e. GPR) which allow a high-resolution mapping of active layer conditions are desired. Fig.5 illustrates active layer depth in each point during the early freezing periods. The recorded values range from 1.92m to 2.44m, which nearly coincide to the former conclusion [22], and the maximum value of 2.44m was detected at the 10th CMP point, which is about 3Km from the top of the hill and locates near a rather smaller stream but can't be seen in the sketch map of Fig1. The thawing depth varies with topography. For instance, the thickness is getting thinner with downslope in part I. But during the next two parts (II and III), it becomes relatively increasing along the survey. The potential explanation could be inferred from local microclimate, microtopography, hydrology, substrate properties and so on.

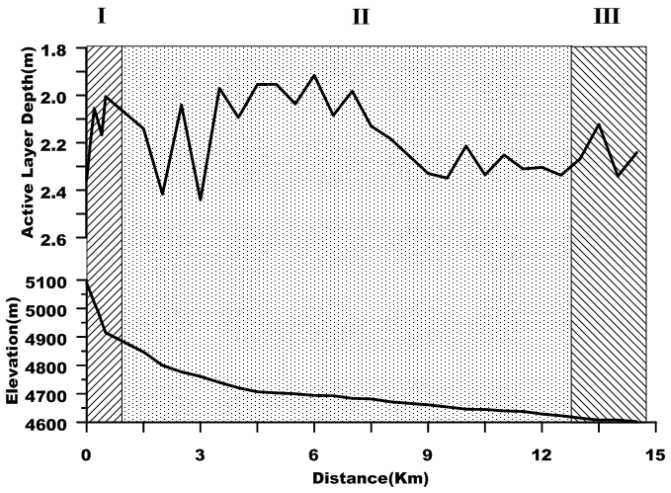

Figure 5. Surface topography and evaluated active layer depth from the entire CMP data during the early freezing periods. The entire survey would be devided into three parts. The first part is "I", which ranges from No. 1 to 7 of CMP data and stands for strong hillslope; the second part is "II", which ranges from No. 8 to 27 of CMP data and delegates slightly weak hillslope; the last one is "III", which ranges from No. 28 to 32 of CMP data and relates to a seasonal stream.

IV. CONCLUSIONS

High-frequency ground-penetrating radar was applied at a permafrost site (viz. Amdo) of central Tibetan Plateau in order to explore the spatial distribution about soil water content and active layer depth during the early freezing periods. Although experimental observation was conducted within a rather small spatial scale with variable topography and soil textures, this investigation implies the potential of multi-offset ground-penetrating radar to efficiently and non-invasively evaluate soil water content and active layer depth with high spatial resolution. Compared with traditional methods like time domain reflectometry (TDR) or gravimetric sampling, ground-penetrating radar (GPR) technique is more reliable and convenient in terms of observing time and cost [23]., .

During this survey, a reflection profile and thirty-two common-mid point (CMP) soundings were performed together along with the whole survey by using 250MHz GPR technique. Corresponding volumetric soil water content and active layer depth measurements revealed spatial variation and heterogeneity in the experimental basin. The topography (i.e. slope and elevation) and stream distribution significantly alter spatial pattern of soil moisture and active layer thickness in the Amdo catchment, located in central Tibetan Plateau.

ACKNOWLEDGEMENT

This study was funded by the Major State Basic Research Development Program of China (973 Program) under grant Nos. 2010CB951701 and 2010CB428606 and by the National Science Foundation of China (No. 595 40775045 and No. 41071042), also supported by the Innovation Project of the Chinese Academy of Sciences (KZCX2-YW-BR-22).

REFERENCES

[1] A. Neal, "Ground-penetrating radar and its use in sedimentology: principles, problems and progress", Earth-Science Reviews, vol.66, pp.261-330, 2004.

[2] J.A.Doolittle, B.Jenkinson, D.Hopkins, M.Ulmer and W.Tuttle, "Hydropedological investigations with ground-penetrating radar (GPR): Estimating water table depths and local ground-water flow pattern in areas of coarse-textured soils", Geoderma, vol.131, pp.317-329, 2006.

[3] K.M. Hinkel, J.A. Doolittle, J.G. Bockheim, F.E. Nelson, R. Paetzold, J.M. Kimble and R. Travis, "Detection of subsurface permafrost features with ground-penetrating radar, Barrow, Alaska", Permafrost and Periglacial Processes, vol.12, pp.179-190, 2001.

[4] J.A. Huisman, S.S. Hubbard, J.D. Redman and A.P. Annan, "Measuring soil water content with ground penetrating radar: A review", Vadose Zone Journal, vol.2, pp. 476-491, 2003.

[5] I.A. Lunt, S.S. Hubbard and Y. Rubin, "Soil moisture content estimation using ground-penetrating radar reflection data", Journal of Hydrology, vol.307, pp.254-269, 2005.

[6] C.M. Steelman and A.L. Endres, "Comparison of petrophysical relationships for soil moisture estimation using GPR ground waves", Vadose Zone Journal, vol.10, pp. 270-285, 2010.

[7] T. Wu, S. Li, G. Cheng and Z. Nan, "Using ground-penetrating radar to detect permafrost degradation in the northern limit of permafrost on the Tibetan Plateau", Cold Regions Science and Technology, vol.41, pp. 211-219, 2005.

[8] L. Zhao, Q. Wu, S.S. Marchenko and N. Sharkhuu, " Thermal state of permafrost and active layer in central Asia during the international polar year", Permafrost and Periglacial Processes, vol.21, pp.198-207, 2010.

[9] S.A. Arcone, D.E. Lawson, A.J. Delaney, J.C. Strasser and J.D. Strasser, "Ground-penetrating radar reflection profiling of groundwater and bedrock in an area of discontinuous permafrost", Geophysics, vol.63, pp. 1573-1584, 1998.

[10] G. Gacitua, M.P. Tamstorf, S.M. Kristiansen and J.A. Uribe, "Estimations of moisture content in the active layer in an Arctic ecosystem by using ground-penetrating radar profiling", Journal of Applied Geophysics, doi: 10.1016/j.jappgeo.2011.12.003, 2011.

[11] U. Wollschlager, H. Gerhards, Q. Yu, and K. Roth, "Multi-channel ground-penetrating radar to explore spatial variations in thaw depth and moisture content in the active layer of a permafrost site", The Cryosphere, vol.4, pp. 269-283, 2010.

[12] Y. Zhang, T. Ohata and T. Kadota,"Land-surface hydrological processes in the permafrost region of the eastern Tibetan Plateau", Journal of Hydrology, vol.283, pp.41-56, 2003.

[13] M.Yang, T.Yao, X. Gou, T. Koike and Y. He,"The soil moisture distribution, thawing-freezing processes and their effects on the seasonal transition on the Qinghai-Xizang (Tibetan) plateau", Journal of Asian Earth Sciences, vol.21, pp.457-465, 2003.

[14] C.M. Steelman and A.L. Endres, "An examination of direct ground wave soil moisture monitoring over an annual cycle of soil conditions", Water Resources Research, vol.46, Wl1533, 2010.

[15] C.M. Steelman and A.L. Endres, "Evolution of high-frequency ground-penetrating radar direct ground wave propagation during thin frozen soil layer development", Cold regions science and technology, vol.57, pp.116-122, 2009.

[16] G.C. Topp, J.L. Davis and A.P. Annan, "Electromagnetic determination of soil water content: Measurement in coaxiale transmission lines", Water Resources Research, vol.16, pp.574-582, 1980.

[17] K. Roth, R. Schulin, H. Fluhler and W. Attinger, "Calibration of time domain reflectometry for water content measurement using a composite dielectric approach", Water Resources Research, vol.26, pp.2267-2273, 1990.

[18] A. Rodhe and J. Seibert, "Groundwater dynamics in a till hillslope: flow directions, gradients and delay", Hydrological Processes, vol.25, pp.1899-1909, 2011.

[19] J.A. Heginbottom, "Permafrost mapping: a review", Progress in Physical Geography, vol.26, pp. 623-642, 2002.

[20] H.M. French, "The periglacial environment, third edition", Wiley, pp.458, 2007.

[21] R.V. Everdingen, "Multi-language glossary of permafrost and related ground-ice terms. National Snow and Ice Data Center/World Data Center for Glaciology, Boulder, CO, http://nsidc.org/fgdc/glossary/, 1998", revised May 2005.

[22] Q. Wu, Z. Lu, Y. Liu, "Permafrost changes in the Tibetan Plateau", Advances in climate change research, Article ID: 1673-1719, 2006.

[23] J.A. Huisman, C. Sperl, W. Bouten and J.M. Verstraten, "Soil water content measurements at different scales: accuracy of time domain reflectometry and ground-penetrating radar", Journal of Hydrology, vol.245, pp.48-58, 2001.